

RADIATIVE SIGNATURES OF RELATIVISTIC SHOCKS

JOHN G. KIRK AND BRIAN REVILLE

Max-Planck-Institut für Kernphysik, Postfach 10 39 80, 69029 Heidelberg, Germany

To appear in ApJ Letters

ABSTRACT

Particle-in-cell simulations of relativistic, weakly magnetized collisionless shocks show that particles can gain energy by repeatedly crossing the shock front. This requires scattering off self-generated small length-scale magnetic fluctuations. The radiative signature of this first-order Fermi acceleration mechanism is important for models of both the prompt and afterglow emission in gamma-ray bursts and depends on the strength parameter $a = \lambda e|\delta B|/mc^2$ of the fluctuations (λ is the length-scale and $|\delta B|$ the magnitude of the fluctuations.) For electrons (and positrons), acceleration saturates when the radiative losses produced by the scattering cannot be compensated by the energy gained on crossing the shock. We show that this sets an upper limit on both the electron Lorentz factor: $\gamma < 10^6 (n/1\text{ cm}^{-3})^{-1/6} \bar{\gamma}^{1/6}$ and on the energy of the photons radiated during the scattering process: $\hbar\omega_{\max} < 40 \text{ Max}(a, 1) (n/1\text{ cm}^{-3})^{1/6} \bar{\gamma}^{-1/6} \text{ eV}$, where n is the number density of the plasma and $\bar{\gamma}$ the thermal Lorentz factor of the downstream plasma, provided $a < a_{\text{crit}} \sim 10^6$. This rules out ‘jitter’ radiation on self-excited fluctuations with $a < 1$ as a source of gamma-rays, although high-energy photons might still be produced when the jitter photons are upscattered in an analog of the synchrotron self-Compton process. In fluctuations with $a > 1$, radiation is generated by the standard synchrotron mechanism, and the maximum photon energy rises linearly with a , until saturating at 70 MeV, when $a = a_{\text{crit}}$.

Subject headings: radiation mechanisms: non-thermal — acceleration of particles — gamma rays: bursts

1. INTRODUCTION

In astrophysics, the most widely discussed mechanism of particle acceleration is the first-order Fermi process operating at collisionless shocks. It is based on the idea that particles undergo stochastic elastic scatterings both upstream and downstream of the shock front. This causes particles to wander across the shock repeatedly. On each crossing, they receive an energy boost as a result of the relative motion of the upstream and downstream plasmas. At non-relativistic shocks, scattering causes particles to diffuse in space, and the mechanism, termed ‘diffusive shock acceleration’, is widely thought to be responsible for the acceleration of cosmic rays in supernova remnants. At relativistic shocks, the transport process is not spatial diffusion, but the first-order Fermi mechanism operates nevertheless (for reviews see Kirk & Duffy 1999; Hillas 2005). In fact, the first *ab initio* demonstrations of this process using particle-in-cell (PIC) simulations have recently been presented for the relativistic case (Spitkovsky 2008b; Martins et al. 2009; Sironi & Spitkovsky 2009).

Several factors, such as the lifetime of the shock front, or its spatial extent, can limit the energy to which particles can be accelerated in this process. However, even in the absence of these, acceleration will ultimately cease when the radiative energy losses that are inevitably associated with the scattering process overwhelm the energy gains obtained upon crossing the shock. Exactly when this happens depends on the details of the scattering process.

In the non-relativistic case, the diffusion coefficient

john.kirk@mpi-hd.mpg.de

is frequently parameterized in terms of its lower limit, known as Bohm diffusion, at which the particle mean free path equals the gyro radius. In this case, particles that achieve the highest possible energy radiate synchrotron photons up to an energy $\sim 150\eta(v_s/c)^2$ MeV, where v_s is the speed of the shock front and $\eta(\leq 1)$ is the inverse ratio of the diffusion coefficient to its value in the Bohm limit. Interestingly, this photon energy is independent of the magnetic field strength.

In PIC simulations of weakly magnetized shocks, however, particles appear to undergo small-angle scatterings on fluctuations in the electromagnetic fields that are driven by the Weibel instability. These have a length scale roughly equal to the inertial length c/ω_p , where $\omega_p = \sqrt{4\pi ne^2/\bar{\gamma}m}$ is the relativistic electron plasma frequency, and $\bar{\gamma}$ is the Lorentz factor of the average thermal motion. As we show below (see Eq. (6)) the resulting mean free path of a particle of Lorentz factor γ is proportional to γ^2 , rather than the linear dependence expected in Bohm diffusion. This modifies the maximum energy of the synchrotron photons (Derishev 2007), but the radiation emitted when a particle is deflected through very small angles differs significantly from synchrotron radiation (Landau & Lifshitz 1975), and can, in principle, produce more energetic photons. This has led to the suggestion that “jitter” radiation from shock-accelerated particles is responsible for both the prompt emission (Medvedev 2006) and the afterglow (Medvedev et al. 2007) from gamma-ray bursts. In this *Letter* we show that the inherent weakness of the scattering produced by Weibel-driven turbulence implies that radiation losses quench first-order Fermi acceleration relatively quickly.

In this case, the maximum photon energy is given by (16) and particles are unable to produce X-ray or gamma-ray photons in the downstream rest frame.

2. RELATIVISTIC SHOCK FRONTS

Recent particle-in-cell simulations of relativistic shocks have revealed fundamental differences between the magnetized and unmagnetized cases. The most detailed results are available for electron-positron pair plasmas, which are likely to be found in gamma-ray bursts and pulsar winds. The upstream and downstream plasmas can be characterized by magnetic field strengths $B_{u,d}$ and number densities $n_{u,d}$ measured in the respective rest frames. The upstream plasma is cold, and streams into the shock with a Lorentz factor $\bar{\gamma}$, roughly equal to the thermal Lorentz factor of the downstream plasma. The magnetization parameters in each region can be written:

$$\begin{aligned}\sigma_u &= B_u^2/(4\pi n_u m c^2) \\ \sigma_d &= B_d^2/(4\pi \bar{\gamma} n_d m c^2)\end{aligned}\quad (1)$$

At a parallel shock, $B_u = B_d$ and $\sigma_d \ll \sigma_u$. If the magnetic field is compressed at an oblique shock front, one expects $\sigma_u \sim \sigma_d$, since $B_d/B_u \sim n_d/n_u \sim 3\bar{\gamma}$. However, if magnetic field is generated, then $\sigma_d \gg \sigma_u$. It is found (Sironi & Spitkovsky 2009) that ‘unmagnetized’ shocks, with $\sigma_u < 10^{-3}$, are mediated by the Weibel instability. This is true also for shocks with an upstream magnetic field parallel to the shock normal, provided $\sigma_u < 0.1$. On the other hand, more strongly magnetized or oblique shocks are mediated by the synchrotron maser instability that operates when particles streaming into the shock start to gyrate about the compressed downstream magnetic field. In each case, it is possible to estimate a length scale on which turbulence is initially generated in the electromagnetic field. For Weibel-mediated (unmagnetized) shocks, this is

$$\lambda_w = \ell_w c / \omega_p \quad (2)$$

with $\ell_w \sim 10$, according to Sironi & Spitkovsky (2009). Here, ω_p is the local plasma frequency. Because $n_d/n_u \sim \bar{\gamma}$, the plasma frequencies in the upstream and downstream media are roughly equal, and so the wavelength of the turbulence generated is approximately the same. For the purpose of estimating radiative signatures of accelerated particles, it is more convenient to characterize the fluctuations in terms of their ‘strength’, or ‘wiggler’ parameter a , defined as the ratio of their length scale to the length defined by the turbulent field strength: $a = \lambda e |\delta B| / mc^2$. In the upstream and downstream media (subscripts “u” and “d”) one has

$$\begin{aligned}a_{w,u} &\approx \ell_w \sigma_u^{1/2} \\ a_{w,d} &\approx \ell_w \bar{\gamma} \sigma_d^{1/2}\end{aligned}\quad (3)$$

This suggests that for Weibel-mediated shocks in pair plasmas the strength parameters are likely to be small ($a \lesssim 1$), although moderate values ($a \gtrsim 1$) are possible if the self-generated field grows locally to levels close to equipartition. Carrying out the same analysis for unmagnetized electron-ion shocks results in an additional factor of (m_i/m_e) in the value of the strength parameter, since the dominant length-scale in this case is the ion skin-depth (Spitkovsky 2008a). Provided $\sigma_{u,d} \ll 1$, moderate strength parameters can still be expected.

For magnetized shocks mediated by the synchrotron maser instability (Lyubarsky 2006), the characteristic length in the downstream plasma $\lambda_{s,d}$ is dictated by the requirement that the incoming particles be significantly deflected:

$$\lambda_{s,d} = \ell_s \bar{\gamma} m c^2 / e B_d \quad (4)$$

with $\ell_s \sim 1$. This generates electromagnetic waves of strength parameter

$$a_{s,d} = \ell_s \bar{\gamma} \quad (5)$$

These waves propagate into the upstream medium without change of their (Lorentz invariant) strength parameter: $a_{s,u} = a_{s,d}$.

To summarize, the strength parameters associated with shock-generated turbulence are likely to be small ($a \lesssim 1$) in the case of Weibel-mediated pair shocks, but moderate $a \sim \bar{\gamma}$ in the case of electron-ion shocks and magnetized shocks mediated by the synchrotron instability.

3. PARTICLE ACCELERATION

Fermi acceleration at relativistic shocks differs from that at nonrelativistic shocks in that it is sensitive to the physics of the particle scattering process (e.g., Kirk & Duffy 1999). Typically, it is assumed that the particles undergo stochastic small-angle deflections through interactions with magnetic irregularities. According to the strength parameter of these irregularities, the transport of the particles can then be divided into two distinct regimes, which we call ‘ballistic’ and ‘helical’. In ballistic transport, the scattering mean free path is shorter than the gyroradius in the local field, so that the curvature radius of a trajectory is larger than the length scale on which this quantity fluctuates. This kind of transport is produced by fluctuations with $a < \gamma$. On the other hand, in the helical transport regime, gyro motion is only slightly perturbed. Particles have sufficient time to gyrate about the field while their pitch angles and guiding-center positions diffuse. This requires fluctuations with $a > \gamma$. This has a strong influence on the acceleration process and its interplay with radiation losses.

3.1. Ballistic transport regime

At a relativistic shock, a particle remains in the upstream medium until it has been deflected, on average, through an angle of $1/\bar{\gamma}$ in the upstream rest frame. A turbulent fluctuation of strength parameter a , deflects a particle of Lorentz factor γ through an angle a/γ . Provided this angle is small, the diffusion coefficient is simply $D_\theta = a^2 \nu_{sc} / \gamma^2$, where ν_{sc} is the mean scattering frequency. The average number of scatterings in the upstream medium between shock encounters is therefore

$$N_{\text{scatt},u} \approx (\gamma/a_u \bar{\gamma})^2 \quad (6)$$

At each scattering, the power radiated in photons by the energetic particle can be estimated from Larmor’s formula:

$$\left. \frac{\Delta\gamma}{\gamma} \right|_{\text{loss},u} \approx \frac{2a_u^2 e^2 \gamma}{3mc^2 \lambda_u} \quad (7)$$

assuming inverse Compton losses can be neglected. For kinematic reasons, the average energy gain per cycle is

roughly a factor of two (Achterberg et al. 2001), so that the acceleration process will saturate when the energy lost in the upstream medium is roughly γmc^2 . This implies $N_{\text{scatt},u} \Delta\gamma/\gamma|_{\text{loss},u} < 1$, or

$$\gamma < \left(\frac{3mc^2\lambda_u\bar{\gamma}^2}{2e^2} \right)^{1/3} \quad (8)$$

Applying the same argument, energy loss by scattering in the downstream medium, where particles must be scattered through an angle of roughly $\pi/2$, imposes the condition

$$\gamma < \left(\frac{3mc^2\lambda_d}{2e^2} \right)^{1/3} \quad (9)$$

which, since $\lambda_d \sim \lambda_u$, is more restrictive.

The ballistic regime requires $a_{u,d} < \gamma$, which, according to (3), is fulfilled for unmagnetized pair shocks for all particles with $\gamma > \bar{\gamma}$, provided $\ell_w \lesssim 10$, and $\sigma_{u,d} < 1$. For electron-ion shocks, this condition is unlikely to be satisfied for electrons with $\gamma \sim \bar{\gamma}$, but is easily satisfied for electrons that achieve energies comparable to those of thermal ions or higher, provided $\sigma_{u,d} \ll 1$.

3.2. Helical transport regime

In the helical transport regime, energy losses are important at all points along a trajectory, and, if Bohm diffusion operates, the time taken to return to the shock front is approximately the gyro period. Under these conditions, the maximum Lorentz factor has been calculated by Achterberg et al. (2001):

$$\gamma < \frac{3m^2c^3}{2e^3B} \quad (10)$$

At magnetized, relativistic shocks, particle acceleration by the first-order Fermi mechanism is less plausible, since, at least for superluminal shocks, it relies on strong cross-field diffusion (e.g., Baring & Summerlin 2009). However, if the process does operate, particles can move out of the helical regime into the ballistic regime, as their Lorentz factor increases. Because of this, it is convenient to define a critical strength parameter a_{crit} such that when $a = a_{\text{crit}}$ the maximum Lorentz factor γ_{max} permitted by radiation losses is achieved just at the point at which the transport changes character from helical to ballistic. If $a > a_{\text{crit}}$, all particles remain in the helical regime. On the other hand, if $a < a_{\text{crit}}$, particles of the maximum Lorentz factor undergo ballistic transport, but lower energy particles may be in the helical regime. Since the transition from helical to ballistic occurs at $\gamma = a$, the critical strength parameter in the downstream region follows from (9):

$$a_{\text{crit}} = \left(\frac{3mc^2\lambda_d}{2e^2} \right)^{1/3} \quad (11)$$

Expressed in these terms, the maximum Lorentz factor in the helical transport regime (10) is $\gamma_{\text{max}} = \sqrt{a_{\text{crit}}^3/a}$. Typically, $a_{\text{crit}} \gg 1$ in both unmagnetized and magnetized shocks: inserting, for example, the length scale appropriate for Weibel-mediated shocks (2) one finds

$$a_{\text{crit}} = 1.4 \times 10^6 \ell_w^{1/3} \bar{\gamma}^{1/6} (n/1 \text{ cm}^{-3})^{-1/6} \quad (12)$$

In the helical regime, the first-order Fermi process has been observed, so far, only in PIC simulations of subluminal pair shocks (Sironi & Spitkovsky 2009). The failure of the mechanism at superluminal shocks may be because the helical character of orbits prevents particles from recrossing the shock front by sweeping them away into the downstream medium (Begelman & Kirk 1990; Bednarz & Ostrowski 1996; Lemoine et al. 2006). However, first-order Fermi is not the only possible acceleration mechanism at superluminal shocks. Strong electromagnetic wave fields are generated at these shocks, and, at least in plasmas that contain some protons, these are thought to be responsible for particle acceleration (Amato & Arons 2006; Lyubarsky 2006). This can only happen if the nonthermal particles are confined within the source, i.e., if they are deflected through an angle ~ 1 before losing their energy to radiation. In this case, demanding that a particle be able to complete a gyration before radiating its energy leads to the same constraint as obtained for first order Fermi acceleration (10).

Combining the constraints from the ballistic regime (9) and the helical regime (10) gives:

$$\gamma_{\text{max}} = \begin{cases} a_{\text{crit}} & \text{for } a < a_{\text{crit}} \\ a_{\text{crit}}\sqrt{a_{\text{crit}}/a} & \text{for } a > a_{\text{crit}} \end{cases} \quad (13)$$

4. RADIATIVE SIGNATURES

The spectrum of photons that are emitted when a particle is scattered by turbulent fluctuations is, in the general case, quite complex (Toptygin & Fleishman 1987). However, to estimate the radiative signature of a particle accelerated at a relativistic shock front several simplifications can be made.

Consider the radiation emitted when a particle is scattered by a single fluctuation of length λ and strength parameter a , and is unperturbed before and after interaction. The character of the emission depends crucially on the “formation” or “coherence” length of the radiated photons Akhiezer & Shul’ga (1987). At low frequencies, this length becomes large, but we confine our estimates to the highest frequency photons produced in the interaction. If $a > 1$, the formation length is roughly $\lambda_{\text{coh}} \approx mc^2/eB$. This is much smaller than the wavelength of the turbulence, so that the individual photons are created in regions in which the field is almost constant and homogeneous. The result is synchrotron radiation, with the emissivity defined by the local value of the field. The emission extends up to the roll-over frequency of the highest energy electrons:

$$\omega_{\text{max}} \approx 0.5\gamma_{\text{max}}^2 eB/mc = 0.5a\gamma^2 c/\lambda \quad \text{for } a > 1 \quad (14)$$

These photons are radiated into a forward directed cone of opening angle $1/\gamma$. Well below this frequency, the emissivity is proportional to $\omega^{1/3}$, provided the coherence length remains shorter than the wavelength of the turbulence.

If, on the other hand, $a < 1$, the particle is deflected through an angle that is small compared to $1/\gamma$. In this case, the coherence length is no longer limited by deflection, but is given by the distance moved by the par-

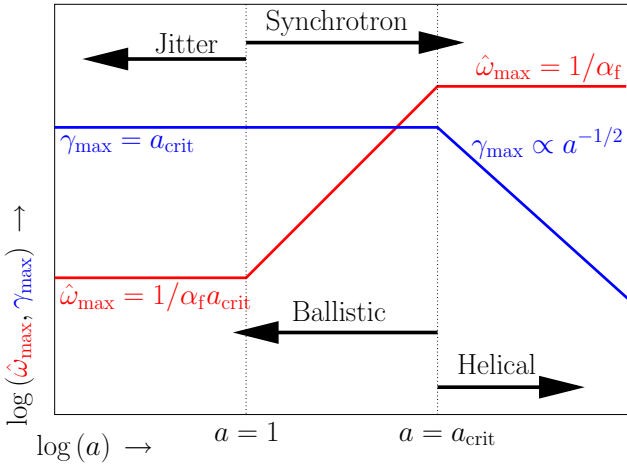


FIG. 1.— The maximum Lorentz factor γ_{\max} of electrons and the maximum photon energy $\hat{\omega}_{\max} = \hbar\omega_{\max}/mc^2$ they radiate when scattered by magnetic fluctuations of strength a (see Eqs. (3) and (5)) at a relativistic shock. The critical strength parameter a_{crit} is defined in (12), α_f is the fine-structure constant. The jitter/synchrotron regimes are separated by the vertical $a = 1$ line; the ballistic/helical transport regimes by the $a = a_{\text{crit}}$ line. See the electronic edition of the Journal for a color version of this figure.

icle in the lab. frame during the time it takes for the photon to move one wavelength ahead of the particle: $\lambda_{\text{coh}} \approx \gamma^2 c/\omega$. The spectrum of radiated photons rolls over when $\lambda_{\text{coh}} \approx \lambda$, and is flat ($\propto \omega^0$) towards lower frequency, as in the case of bremsstrahlung. The maximum frequency is roughly

$$\omega_{\max} \approx 0.5 \gamma_{\max}^2 c / \lambda \quad \text{for } a < 1 \quad (15)$$

In each case, most of the power radiated by an individual electron emerges within a decade of the roll-over frequency that corresponds to its Lorentz factor. Therefore, to estimate the spectrum radiated by a power-law distribution of electrons, with differential number density $dn/d\gamma \propto \gamma^{-p}$, one can simply make a one-to-one correspondence between radiated frequency and Lorentz factor: $\omega = \text{Max}(a, 1)\gamma^2 c / \lambda$. Larmor's formula, which holds for all values of a , states that the radiated power is proportional to the Lorentz factor squared, so that the power radiated by dn electrons of Lorentz factor γ is $dL \propto \gamma^2 dn$. A simple change of variables then shows that in both the synchrotron and jitter cases, the spectrum at frequencies below the roll-over frequency of the highest energy electrons is $dL/d\omega \propto \omega^{-(p-1)/2}$.

Combining the limit on the Lorentz factor (9) with the expressions for the roll-over frequency (14) and (15), one finds for the maximum frequency that can be radiated by particles accelerated at a relativistic shock front:

$$\frac{\hbar\omega_{\max}}{mc^2} = \begin{cases} (\alpha_f a_{\text{crit}})^{-1} & a < 1 \\ a(\alpha_f a_{\text{crit}})^{-1} & 1 < a < a_{\text{crit}} \\ \alpha_f^{-1} & a > a_{\text{crit}} \end{cases} \quad (16)$$

where $\alpha_f = e^2/\hbar c$ is the fine structure constant. There are two transport regimes: that in which the unperturbed motion of the highest energy particles is ballistic ($a < \gamma_{\max}$) and that in which it is helical ($a > \gamma_{\max}$) and

two radiation regimes: those of jitter ($a < 1$) and synchrotron ($a > 1$) radiation. This is illustrated in Fig. 1.

5. DISCUSSION

Radiation emitted by relativistic electrons scattering in the small-scale turbulent magnetic fields generated at Weibel-mediated relativistic shocks has been proposed as the mechanism responsible for both the prompt and afterglow emission of gamma-ray bursts (Medvedev 2006; Medvedev et al. 2007). The evidence in favour of this suggestion is based on modelling the observed spectra assuming an electron distribution of power-law type with arbitrary high and low energy cut-offs. Power-law distributions are expected on theoretical grounds (Achterberg et al. 2001; Kirk et al. 2000), and are indeed observed in simulations of weakly magnetized, relativistic shocks (Spitkovsky 2008b; Sironi & Spitkovsky 2009; Martins et al. 2009). However, the constraint on the maximum photon energy imposed by the above analysis (16) suggests that this picture is not self-consistent, because the scatterings are too weak to accelerate electrons to the required Lorentz factor. In order to radiate photons of energy $\sim mc^2$ in the plasma rest frame, strong fluctuations of large length-scale with $a \sim \alpha_f a_{\text{crit}} \sim 10^4$ are required.

The above conclusion rests on the assumption that the same fluctuations are responsible for both the particle transport and radiation. In terms of the strength parameter a and length scale λ that we use to characterize the fluctuations, the deflection angle scales as $\Delta\theta \propto a$ and the radiation losses as $\Delta\gamma \propto a^2/\lambda$. If, therefore, the scattering responsible for isotropization occurs on fluctuations of comparable strength, but much larger length scale than those responsible for the radiation losses, the limit on the maximum photon energy (16) is relaxed. In principle, the fluctuations induced by the Weibel instability could be responsible for photon production, provided longer wavelength fluctuations are present to provide the necessary isotropization and transport. The accelerated particles themselves appear to generate longer wavelength fluctuations downstream of the shock (Keshet et al. 2009), but this is a relatively small effect compared to that needed to significantly influence the maximum photon energy.

On the other hand, if, as simulations suggest, the Weibel-induced fluctuations are responsible for the transport, the bulk of the radiation must be produced by interaction with fluctuations of much shorter wavelength. An obvious candidate is the soft photon field produced by the interaction of thermal electrons with the Weibel-induced fluctuations — the ‘jitter’ analog of the synchrotron photons produced by relativistic thermal electrons (Baring & Braby 2004; Giannios & Spitkovsky 2009). With these photons as targets, the radiation mechanism is analogous to the synchrotron self-Compton mechanism, which has been discussed in connection with the problem of rapidly decaying magnetic fluctuations (Rossi & Rees 2003). While this model offers a simple explanation for the production of high energy photons, it does not easily accommodate those low-frequency BATSE burst spectra (Baring & Braby 2004), that violate the so-called synchrotron ‘line of death’ (Preece et al. 1998). These rare cases might be accounted for if the upscattering occurs

deep in the Klein-Nishina regime (Derishev et al. 2001; Bošnjak et al. 2009), an explanation which is facilitated if the target photons arise not from synchrotron emission, but from relatively hard jitter radiation.

This research was supported in part by the National Science Foundation under Grant No. PHY05-51164. BR gratefully acknowledges support from the Alexander von

REFERENCES

- Achterberg, A., Gallant, Y. A., Kirk, J. G., & Guthmann, A. W. 2001, MNRAS, 328, 393
- Akhiezer, A. I., & Shul'ga, N. F. 1987, Soviet Physics Uspekhi, 30, 197
- Amato, E., & Arons, J. 2006, ApJ, 653, 325
- Baring, M. G., & Braby, M. L. 2004, ApJ, 613, 460
- Baring, M. G., & Summerlin, E. J. 2009, ArXiv e-prints
- Bednarz, J., & Ostrowski, M. 1996, MNRAS, 283, 447
- Begelman, M. C., & Kirk, J. G. 1990, ApJ, 353, 66
- Bošnjak, Ž., Daigne, F., & Dubus, G. 2009, A&A, 498, 677
- Derishev, E. V. 2007, Ap&SS, 309, 157
- Derishev, E. V., Kocharyan, V. V., & Kocharyan, V. V. 2001, A&A, 372, 1071
- Giannios, D., & Spitkovsky, A. 2009, MNRAS, 1310
- Hillas, A. M. 2005, Journal of Physics G Nuclear Physics, 31, 95
- Keshet, U., Katz, B., Spitkovsky, A., & Waxman, E. 2009, ApJ, 693, L127
- Kirk, J. G., & Duffy, P. 1999, Journal of Physics G Nuclear Physics, 25, 163
- Kirk, J. G., Guthmann, A. W., Gallant, Y. A., & Achterberg, A. 2000, ApJ, 542, 235
- Landau, L. D., & Lifshitz, E. M. 1975, The classical theory of fields (Oxford: Pergamon Press, 1975, 4th rev.ed.)
- Lemoine, M., Pelletier, G., & Revenu, B. 2006, ApJ, 645, L129
- Lyubarsky, Y. 2006, ApJ, 652, 1297
- Martins, S. F., Fonseca, R. A., Silva, L. O., & Mori, W. B. 2009, ApJ, 695, L189
- Medvedev, M. V. 2006, ApJ, 637, 869
- Medvedev, M. V., Lazzati, D., Morsony, B. C., & Workman, J. C. 2007, ApJ, 666, 339
- Preece, R. D., Briggs, M. S., Mallozzi, R. S., Pendleton, G. N., Paciesas, W. S., & Band, D. L. 1998, ApJ, 506, L23
- Rossi, E., & Rees, M. J. 2003, MNRAS, 339, 881
- Sironi, L., & Spitkovsky, A. 2009, ApJ, 698, 1523
- Spitkovsky, A. 2008a, ApJ, 673, L39
- . 2008b, ApJ, 682, L5
- Toptygin, I. N., & Fleishman, G. D. 1987, Ap&SS, 132, 213